Available online at www.sciencedirect.com

SCIENCE DIRECT®

Thin Solid Films 469–470 (2004) 404–409

thin solid films

www.elsevier.com/locate/tsf

X-ray characterization of oriented β-tantalum films

Sandeep Kohli[a,*], Patrick R. McCurdy[a], Christopher D. Rithner[a], Peter K. Dorhout[a], Ann M. Dummer[b], Fernando Brizuela[b], Carmen S. Menoni[b]

[a]Department of Chemistry, Colorado State University, Fort Collins CO-80523, United States
[b]NSF Extreme Ultraviolet Science and Technology Center and Department of Electrical Engineering, Colorado State University, Fort Collins CO-80523, United States

Available online 30 October 2004

Abstract

Tantalum (Ta) metal films (10–70 nm) were deposited on a Si(100) substrate with a 500 nm silicon dioxide (SiO_2) interlayer by ion-beam-assisted sputtering. The as-deposited films have been characterized by X-ray diffraction (XRD) and X-ray reflectivity (XRR) techniques. XRD measurements showed the presence of films of the tetragonal phase of tantalum (β-Ta) oriented along the (00l) plane. XRR measurements indicated the presence of graded Ta films, with a thin interface layer between the 500 nm SiO_2 layer and the Ta films. The thickness and density of this interface layer was estimated to be 1.9±0.2 nm and 10.5±0.5 g/cm^3, respectively. X-ray photoelectron spectroscopy (XPS) was used to probe the chemical composition of this interface layer. XPS investigative studies indicated that the interface was likely composed of tantalum silicide ($TaSi_2$) and tantalum silicate ($TaSiO_x$). However, the $TaSiO_x$ layer was reduced during Ar ion sputter depth profile analysis.
© 2004 Elsevier B.V. All rights reserved.

Keywords: X-ray diffraction; X-ray reflectivity; X-ray photoelectron spectroscopy; Tantalum; Sputtering

1. Introduction

Currently, copper metallization is being extensively utilized as an interconnect for Ultra Large Scale Integration (ULSI) applications. However, an underlying layer is necessary for the adhesion of Cu to dielectrics, and more importantly, as a diffusion barrier against the migration of copper ions through the dielectric layer [1]. Tantalum (Ta) metal and Ta–N intermetallics are being used for Cu adhesion and as diffusion barriers. The texture and grain structure of Cu films has been shown to affect the electromigration lifetime of Cu interconnects [2] with that of (111) oriented Cu about four times longer than that of (200) oriented Cu [2]. It has been shown that the growth of Cu(111) is preferred on β-Ta films oriented along (002) crystallographic planes [3].

Despite these and other studies devoted to β-Ta [4–8], the growth mechanism of oriented β-Ta is not clear. There is sufficient lack of information on the related properties of oriented β-Ta/silicon dioxide (SiO_2) and the β-Ta/Si interface. In the present paper, the dual ion beam sputtering deposition technique was used to deposit 10–70 nm tantalum films on Si substrates with a pre-deposited 500 nm SiO_2 layer. X-ray diffraction (XRD), X-ray reflectivity (XRR) and X-ray photoelectron spectroscopy (XPS) techniques were used to investigate the structural and chemical properties of tantalum metal thin films and their interface with the underlying SiO_2 film.

2. Experimental procedure

Films of Ta metal and SiO_2 were deposited using a dual ion beam sputtering deposition technique (Spector IBD system, Veeco) [9]. Ta films (10, 30 and 70 nm) were deposited on the Si (100) substrate pre-coated with a 500 nm SiO_2 layer interlayer. A deposition rate of 0.24 nm/s was achieved using deposition source ion energy of 1250 eV. Base pressure was less than 10^{-3} Pa and chamber temper-

* Corresponding author. Tel.: +1 970 491 4076; fax: +1 970 491 1801.
E-mail address: skohli@lamar.colostate.edu (S. Kohli).

0040-6090/$ - see front matter © 2004 Elsevier B.V. All rights reserved.
doi:10.1016/j.tsf.2004.09.001

ature was ~115 °C. Argon flow rate was held at 36 sccm. XRD and XRR measurements were performed using a Bruker D-8 Discover instrument using Cu K_α radiation (E=8041.3 eV). XPS measurements were performed using a Physical Electronics ESCA 5800 system. Monochromatic Al K_α (E=1486.6 eV), was employed as an X-ray source. The high-resolution XPS scans for chemical state identification were carried out using pass energy of 23.5 eV and step size of 0.1 eV. More details for experimental procedure have been published elsewhere [10,11].

3. Results

The XRD patterns (Fig. 1) of as-deposited 10–70 nm tantalum films indicated the presence of the tetragonal Ta phase (β-Ta) [12] with preferred orientation along (00l). The absence of diffraction peaks other than Ta (002), (004) and (006) indicated the presence of strong texture in these as-deposited films. The Si (400) peak overlapped with (004) reflection from β-Ta. The XRD data from the 10 nm Ta film had a low signal to the noise ratio; however, the Ta (002) peak could be clearly seen. While a peak for tetragonal TaO_2 [13] oriented along (200) could be identified, several other peaks could not even after a thorough scan of the ICDD database for reasonable Ta compounds. The low signal to the noise ratio could be responsible for phase-identification failure. In our as-deposited films, we did not observe any diffraction peaks for the crystalline phases for tantalum oxide, tantalum silicide ($TaSi_2$) or tantalum silicate ($TaSiO_x$) phases.

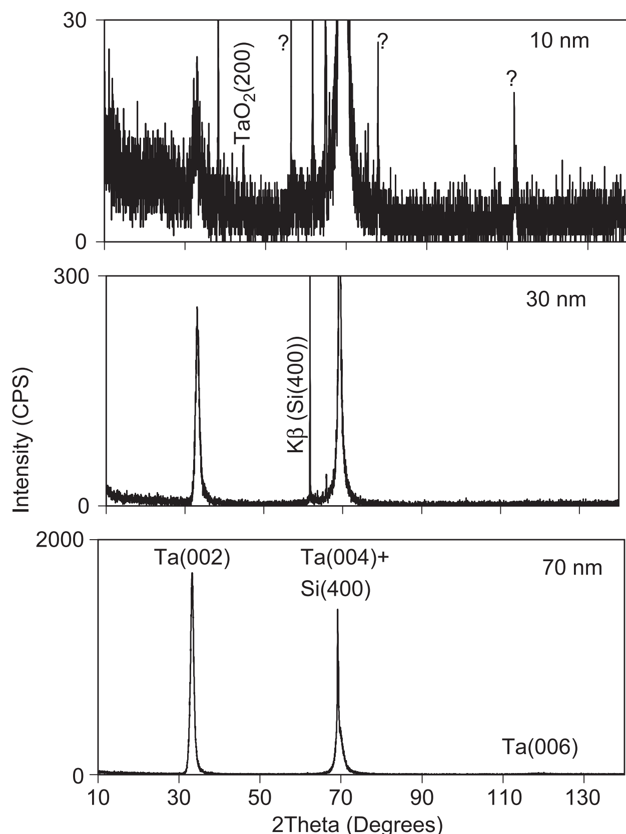

Fig. 1. Theta–2Theta XRD patterns for 10, 30 and 70 nm Ta film deposited on Si(100) substrates with a 500 nm SiO_2 interlayer. Miller indices for Ta and Si diffraction peaks are also shown. Peaks were aligned for maximum Ta (002) signal. Kβ signal from Si(400) is not visible in the XRD spectra for 70 nm due to low signal from Si(400) peak relative to Ta(002).

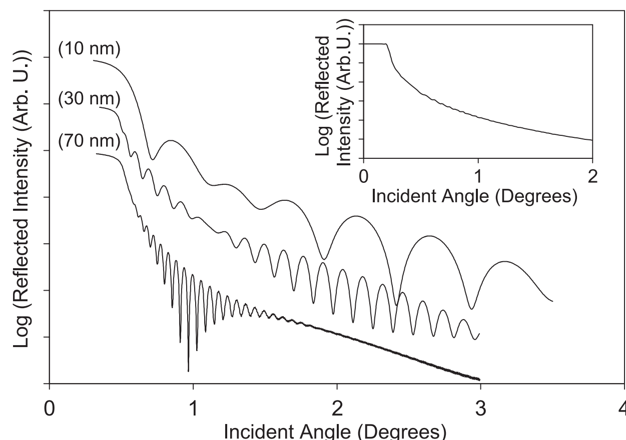

Fig. 2. Experimental XRR curves for 10, 30 and 70 nm Ta films deposited on Si(100) substrates with a 500 nm SiO_2 interlayer. The simulated XRR curve for a 500 nm SiO_2 layer on Si substrate is shown in the inset.

Fig. 2 shows the experimental XRR curves for the as-deposited films. The thickness of SiO_2 was independently verified using spectroscopic ellipsometry and was estimated to be 514 nm. At this thickness, the spacing between the Kiessig [14,15] fringes (used for estimating the thickness) in the XRR curves becomes difficult to resolve; thus the thickness determination was not practically possible. The simulated XRR curve for the 500 nm SiO_2 deposited on Si substrate for Cu K_α radiation using public domain software is shown as inset in Fig. 2 for the sake of comparison[1] [16] Consequently, for the simulation of our XRR curves, the thickness of the SiO_2 film was initially fixed at values obtained from ellipsometry data and any variations in thickness of this layer were ignored. XRR curves for Ta films could not be simulated without the introduction of a thin interface layer between Ta and SiO_2 layers. The results for the thickness and density of Ta are tabulated in Table 1. The thickness and density of this interface layer was found to be 1.9±0.2 nm and 10.5±0.5 g/cm^3, respectively.

Prior to XPS analysis, the adventitious carbon and the native oxide layer on the surface of metal films were removed by Ar ion sputtering to expose the underlying clean surface. Only Ta metal peaks could be seen in the survey XPS spectra of the films deposited on Si substrate with a 500 nm SiO_2 interlayer. XPS Ar ion sputter depth profile analysis was performed on 10–70 nm films. Fig. 3 shows the representative depth profile analysis for the 10

[1] http://cindy.lbl.gov/optical_constants/layer2.html.

Table 1
Simulated X-ray reflectivity results for oriented β-Ta films

Film	Layer materials	Thickness [nm]	Density [g/cm^3]
10 nm Ta	Tantalum	2.3±0.1	14.9±0.3
	Tantalum	5.2±0.1	15.7±0.3
	Interface Layer	1.8±0.1	10.0±0.2
30 nm Ta	Tantalum	2.1±0.1	13.6±0.2
	Tantalum	28.0±0.1	16.0±0.2
	Interface Layer	2.1±0.1	11.0±0.1
70 nm Ta	Tantalum	2.2±0.1	5.4±0.1
	Tantalum	32.3±0.4	16.4±0.2
	Tantalum	36.0±0.4	15.3±0.2
	Interface Layer	1.8±0.1	10.5±0.1

nm Ta film deposited on the Si substrate with a 500 nm SiO_2 interlayer. The presence of oxygen during the start of the sputter profile curves was attributed to the presence of the native oxide layer present at the surface of the tantalum metal film. The appearance of silicon and oxygen peaks after about 4 min of sputtering were attributed to the SiO_2 interlayer. In order to investigate the chemical composition of the interface, detailed analysis of Ta 4f, Si 2p and O 1s spectra after 3–5 min of sputtering was carried out.

The Ta 4f peak fitted spectra after 4.0 min of sputtering showed the presence of metallic Ta $4f_{5/2}$ and $4f_{7/2}$ peaks; 1.91 eV separates the Ta $4f_{5/2}$ and Ta $4f_{7/2}$ in energy while the peak area ratio of 3:4 is expected [17]. These constraints were used in the peak profile modeling. In the absence of the C 1s peak in our spectra, the binding energies of all the elements were normalized against the binding energy of the metallic Ta $4f_{7/2}$ peak that was fixed at 21.64 eV [18,19]. The fitted Ta 4f XPS spectra after 5 min of sputtering (Fig. 5) indicated the presence of additional peaks centered at 26.7 eV (Ta $4f_{7/2}$) and 28.5 eV (Ta $4f_{5/2}$). These peaks could be attributed to the oxide phase of tantalum [19] and were treated with the assumed area ratio of 3:4 as before.

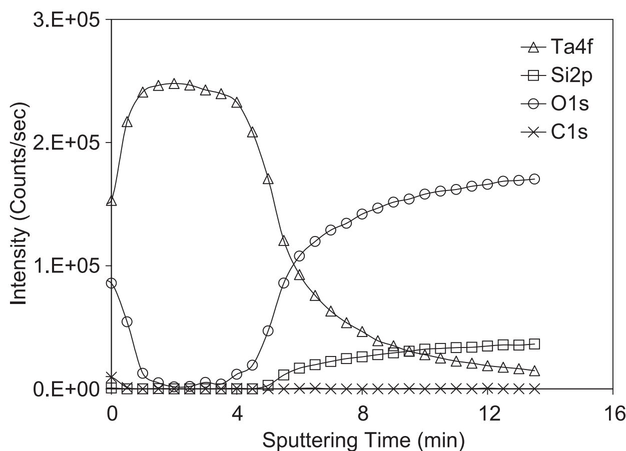

Fig. 3. XPS sputter profile analysis for a 10 nm Ta metal film on a Si(100) substrate with a 500 nm SiO_2 interlayer. The elemental compositions are indicated (Δ) Ta 4f, (□) Si 2p, (○) O 1s and (×) C 1s.

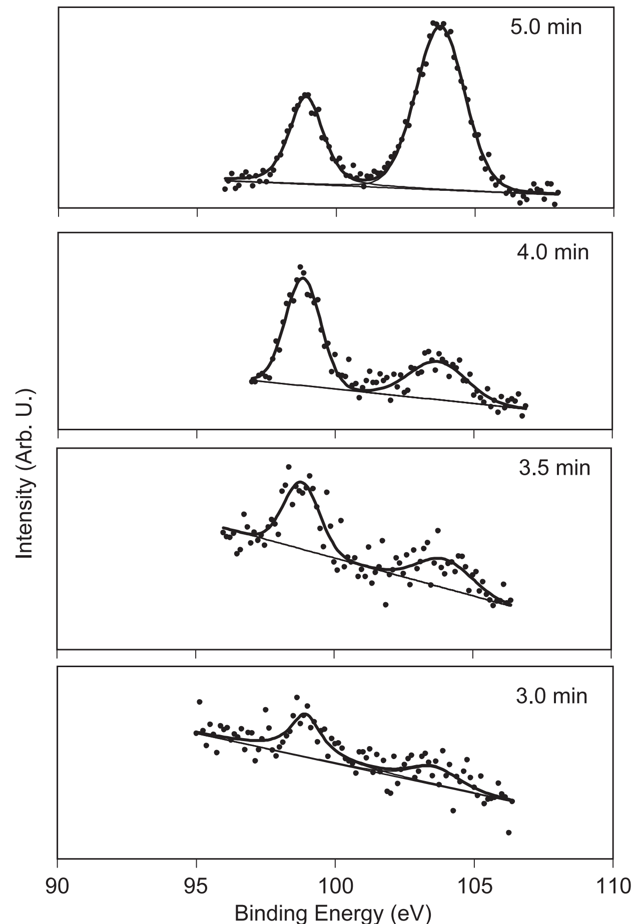

Fig. 4. Experimental and fitted high-resolution Si 2p XPS spectra after the Ta metal film was sputtered for 3–5 min using Ar ions. Dotted points (●●●) are experimental while the heavy solid curve (━) represents the fitted results. The individual peaks are shown as solid curves (—). A Shirley background used is also shown.

The high-resolution fitted spectra for Si 2p peaks are shown in Fig. 4. As seen in the figure, the Si 2p peaks centered on a binding energy of 98.4±0.2 and 103.4±0.2 eV could be seen in all the spectra. The average peak separation between the two peaks remained constant over this sputtering interval (3–5 min) and was found to be 5.0±0.2 eV. Finally, O 1s spectra exhibited the presence of peaks centered on 530.5±0.1 and 531.8±0.3 eV. The average peak separation between the two peaks was found to be 1.3±0.3 eV. Peak positions for different elemental species after 3–5 min of sputtering interval are shown in Table 2.

4. Discussion

Oriented β-Ta films were deposited on Si(100) substrates over a 500 nm SiO_2 interlayer. Formation of tetragonal TaO_2 oriented along (200) in the 10 nm Ta film was possibly due to the surface oxidized oriented β-Ta. The thicknesses of the Ta films were estimated by XRR. While the density of the 70 nm Ta film was similar to the bulk density of Ta metal

Table 2
Peak profile parameters for 10 nm β-Ta films after different sputtering intervals

Sputter time (min)	Peak	Peak position (eV)	Peak separation (eV)	Band FWHM[a] (eV)	FWHM[b] (eV)	% Area
3.0	Ta 4f	21.6	0.0	1.3	1.1	57.1
		23.5	1.9	1.4	1.1	42.9
	Si 2p	98.6	0.0	1.8	1.8	46.3
		103.3	4.7	3.4	3.4	53.7
	O 1s	530.7	0.0	1.6	1.6	56.1
		531.8	1.2	2.7	2.7	43.9
3.5	Ta 4f	21.6	0.0	1.4	1.1	57.1
		23.6	1.9	1.4	1.1	42.9
	Si 2p	98.4	0.0	1.4	1.4	72.8
		103.5	5.1	1.5	1.5	27.2
	O 1s	530.6	0.0	1.2	1.2	18.8
		531.6	1.0	3.4	3.4	81.2
4.0	Ta 4f	21.6	0.0	1.4	1.1	57.1
		23.6	1.9	1.4	1.1	42.9
	Si 2p	98.3	0.0	1.4	1.4	70.1
		103.2	4.9	1.8	1.8	29.9
	O 1s	530.4	0.0	1.2	1.2	22.0
		531.7	1.3	3.0	3.0	78.0
5.0	Ta 4f	21.6	0.0	1.6	1.2	54.1
		23.5	1.9	1.7	1.2	40.6
		26.7	5.0	1.6	0.9	3.0
		28.5	6.9	1.6	1.3	2.3
	Si 2p	98.3	0.0	1.7	1.7	28.8
		103.7	4.8	2.1	2.1	71.2
	O 1s	530.5	0.0	1.7	1.7	22.4
		532.2	1.7	2.2	2.2	77.6

[a] Band FWHM—width of the band at one half its height, in electronvolts.
[b] FWHM—width of the peak component at one half its height, in electronvolts.

(16.7 g/cm^3), the density values for 10 and 30 nm were lower than those reported in literature. This could be due to the increased presence of voids in the 10 and 30 nm films. The presence of a low-density top layer in the simulated film structure could be attributed to the presence of native oxides and surface roughness. However, the low-density layer below the Ta metal film was attributed to the interface layer between the Ta metal and SiO_2 layer. The density of the surface layer for the 70 nm Ta film was considerably lower than those for 10 and 30 nm films. This was possibly due to the increased surface roughness associated with the 70 nm film. Assuming additional Ta metal films with similar densities fit the experimental reflectivity curves better. We considered this to be indicative of graded Ta film.

High-resolution XPS depth profile analysis for 10 nm Ta films (Table 2) shows the presence of Si 2p peaks centered on 98.4±0.2 eV and 103.4±0.2 eV and O 1s peaks centered on 530.5±0.1 and 531.8±0.3 eV. The oxide phase of tantalum could only be observed in sample sputtered for 5 min. The accepted binding energy value for elemental Si $2p_{3/2}$ is 99.79 eV [20] and that for fully oxidized SiO_2 (Si^{4+}) is ~103.5 eV. It has been reported recently that in case of the formation of tantalum silicide ($TaSi_2$) the Si 2p peaks were shifted towards lower energies as compared to bulk elemental silicon and the Ta 4f peak was shifted towards higher binding energy by 0.5 eV as compared to the metallic tantalum [21]. We did not observe any Ta 4f peaks for $TaSi_2$ shifted towards higher energies. The absence of this shifted Ta 4f peak could possibly be due to an overwhelming contribution by metallic Ta 4f peak to the signal. Therefore, it seems that the $TaSi_2$ phase was formed at the β-Ta/SiO_2 interface, as evidenced by the presence of Si 2p peaks shifted towards lower energies as compared to bulk elemental silicon.

The peak at 103.4 eV was attributed to the SiO_2 layer under the tantalum film. The presence of higher binding O 1s peak around 531.8 eV is likely due to SiO_2. The peak seen at lower binding energy of 530.5 eV is usually associated with tantalum oxide [19] and tantalum silicate [22]. The formation of $TaSiO_x$ is usually indicated by the presence of Si 2p peak at 102.1 eV, Ta $4f_{7/2}$ at 26.2 eV [22] (see also Refs. [1,6,17, 18] in Ref. [22]). The peaks for tantalum oxide could only be seen in films sputtered for 5 min. The chemical states associated with this lower binding energy O 1s peak are not clear at this stage. XPS results for 30 and 70 nm Ta film were similar to the results for 10 nm Ta film.

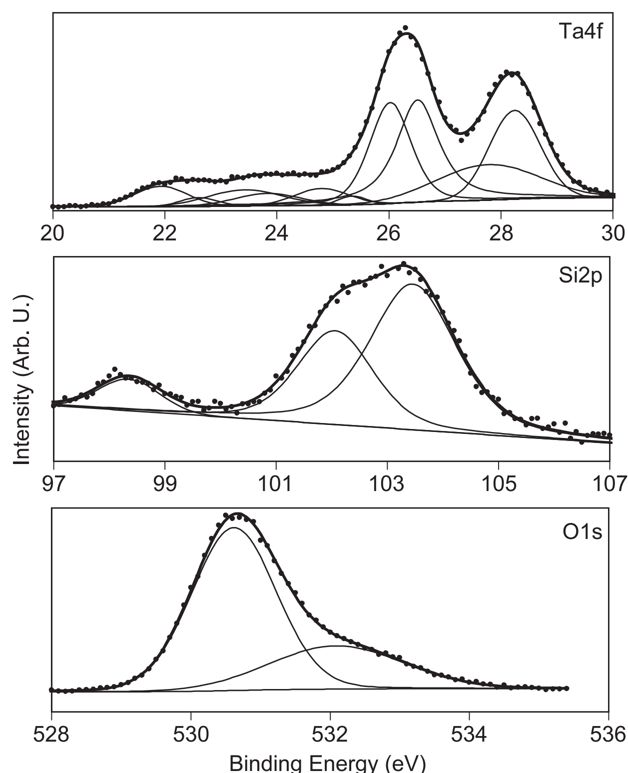

Fig. 5. Experimental and fitted high-resolution Ta 4f, Si 2p, and O 1s XPS spectra for as-deposited 1.0–1.5 nm Ta metal. Dotted points (●●●) are experimental while the heavy solid curve (—) represents the fitted results. The individual peaks are shown as solid curves (—). A Shirley background used is also shown.

Table 3
Chemical state identification of 1.0–1.5 nm Ta films on Si substrate with a 500 nm interlayer

XPS peak	Binding energy (eV)	% Area	FWHM (eV)	Chemical state	
O 1s	530.6	71.2	1.4	TaO_x [19]; Ta_2O_5; [19] $TaSiO_x$ [22]	
	532.1	28.8	2.3	SiO_2 [19]	
Si 2p	102.1	32.5	1.6	$TaSiO_x$ [22]	
	103.5	59.9	1.8	SiO_2 [19]	
	98.3	7.6	1.3	$TaSi_2$ [21]	
Ta 4f	21.9	4.6	1.1	Ta metal [18,19]	$4f_{7/2}$
	23.8	3.4	1.4		$4f_{5/2}$
	22.6	1.4	0.8	$TaSi_2$ [21]	$4f_{7/2}$
	25.3	1.0	0.6		$4f_{5/2}$
	23.4	5.1	1.6	Possibly TaO_x	$4f_{7/2}$
	24.8	3.8	1.1		$4f_{5/2}$
	26	20.5	0.9	TaO_x; $TaSiO_6$ [22]	$4f_{7/2}$
	27.8	15.4	2.2		$4f_{5/2}$
	26.5	25.6	0.9	Ta_2O_5 [19]	$4f_{7/2}$
	28.2	19.2	1.1		$4f_{5/2}$

Despite the results indicating the presence of $TaSi_2$ at the interface, it must be noted that $TaSi_2$ could also be formed during the XPS depth profiling using Ar ions [23]. Also, our XPS depth profile analysis also did not indicate the formation of $TaSiO_x$ that is typically confirmed by the presence of a Si 2p peak at 102.1 eV, a Ta 4f at 26.2 eV and a O 1s peak at 530.6 eV [22]. Preferential sputtering in films with heavy metals is a common problem; hence, it is quite possible that the $TaSiO_x$ phase was reduced during sputter depth profiling. In order to conclusively establish silicide and silicate formation at the interface, it was necessary to probe the film interface without using Ar ion sputter process.

Because XPS is a surface sensitive technique, the XPS signals originate from the top few nanometers of sample. The inelastic mean free path (IMFP) has been defined as the average of the distances, measured along the trajectories, that particles with a given energy travel between inelastic collisions in a substance [24,25]. The estimated value of IMFP for Ta metal, at energies corresponding to Al Kα X-rays is 1.88 nm [26]. Hence, in order to evaluate the interface without sputter depth profile analysis, Ta metal films with thickness of the order of 1.0–1.5 nm were deposited under conditions similar to our 10–70 nm Ta metal films.

The presence of the Si 2*p* peak in the survey XPS spectra for the 1.0–1.5 nm Ta metal film clearly established the fact that we were able to look into the interface below the tantalum metal film without sputtering the metal surface. Si 2p, Ta 4f and O 1s high-resolution XPS spectra are shown in Fig. 5. The binding energies of all the elements were normalized against the binding energy of C 1s peak that was fixed at 284.8 eV. Si 2p spectra showed the presence of peaks at 98.3 eV, 102.0 eV and 103.5 eV. The fitted O 1s spectra showed the presence of peaks at 530.6 eV and 532.1 eV. The fitted Ta 4f spectra showed the presence of metallic and oxidized tantalum films, along with a contribution from silicide and silicate phases. Since the oxidized tantalum was likely due to the presence of native oxide layer present on the surface of the metallic tantalum, the concentration of oxidized tantalum in the Ta 4f spectra was relatively high. The Ta $4f_{7/2}$ peak positions for tantalum metal and Ta_2O_5 reported in NIST database are 21.7 ± 0.2 and 26.5 ± 0.5 eV, respectively, while O 1s binding energy for Ta_2O_5 is 530.3 ± 0.5 eV [19]. The fitted peak parameters and their possible chemical states are presented in Table 3. A detailed comparison of our data with those reported in literature [19,21,22] established that the as-formed β-Ta/SiO_2 interface was comprised of tantalum silicate and silicide phases. This interface was reduced during sputter depth profile analysis using Ar ions, as a result of which the tantalum silicate phase could not be observed during the sputter depth profile XPS analysis.

5. Conclusions

Ion-beam sputter deposited 10–70 nm β-Ta metal films oriented along (00l) were deposited on Si (100) substrate with a 500 nm SiO_2 interlayer. Simulated XRR curves indicate the presence of a 1.9 ± 0.2 nm interface layer with a density of 10.5 ± 0.5 g/cm^3, lying between the graded tantalum metal and SiO_2 interlayer. XPS investigations indicate that the interface was composed of $TaSi_2$, $TaSiO_x$, SiO_2 and Ta_2O_5. Moreover, the $TaSiO_x$ layer was reduced during sputter depth profile analysis using Ar ions.

Acknowledgements

The authors would like to acknowledge the financial support provided by the NSF instrument Grant Nos. NSF-CHE-9808024 and NSF-DMR-0076180. This work was also supported in part by the NSF Engineering Research Centers Program under grant EEC-0310717.

References

[1] S.P. Murarka, S.W. Hymes, Crit. Rev. Solid State 20 (1995) 87.
[2] C. Ryu, K.W. Kwon, A.L.S. Loke, H. Lee, T. Nogami, V.M. Dubin, R.A. Kavari, G.W. Ray, S.S. Wong, IEEE Trans. Electron Devices 46 (1999) 1113.
[3] K.V. Kwon, C. Ryu, R. Sinclair, S.S. Wong, Appl. Phys. Lett. 71 (1997) 3069.
[4] S.L. Lee, D. Windover, T.M. Lu, M. Audino, Thin Solid Films 420 (2002) 287.
[5] J.H. Wang, L.J. Chen, Z.C. Lu, C.S. Hsiung, W.Y. Hsieh, T.R. Yew, J. Vac. Sci. Technol., B 20 (2002) 1522.
[6] L. Gladczuk, C. Joshi, A. Pater, J. Guiheen, Z. Iqbal, M. Sosnowski, Materials Research Society Symposia Proccedings, 2003, p. FF7.2.1.

[7] P.N. Baker, Thin Solid Films 14 (1972) 3.
[8] A.Q. Jiang, A. Yohannan, N.O. Nnolim, T.A. Tyson, L. Axe, S.L. Lee, P. Cote, Thin Solid Films 437 (2003) 116.
[9] C. Montcalm, S.M. Lee, D. Burtner, A. Dummer, D. Siegfried, I. Wagner, M. Watanabe, Annual Technical Conference Proceedings—Society of Vacuum Coaters, 2002, p. 245.
[10] S. Kohli, J.A. Theil, R.D. Snyder, C.D. Rithner, P.K. Dorhout, J. Vac. Sci. Technol., B 21 (2003) 719.
[11] S. Kohli, C.D. Rithner, P.K. Dorhout, J. Appl. Phys. 91 (2002) 1149.
[12] Powder Diffraction File, Joint Committee on Powder Diffraction Standards—International Centre for Diffraction Data, Newton Square, PA., Card No. 25-1280.
[13] Powder Diffraction File, Joint Committee on Powder Diffraction Standards—International Centre for Diffraction Data, Newton Square, PA., Card No. 43-1046.
[14] H. Kiessig, Ann. Phys. 10 (5) (1931) 769.
[15] V.P. Holy, U. Pietsch, T. Baumbach, High-Resolution X-ray Scattering from Thin Films and Multilayers, Springer-Verlag, Berlin, 1999.
[16] B.L. Henke, E.M. Gullikson, J.C. Davis, At. Data Nucl. Data Tables 54 (1993) 181.
[17] D. Briggs, M.P. Seah (Eds.), Practical Surface Analysis: Auger and X-Ray Photoelectron Spectroscopy, John Wiley and Sons, 1996.
[18] J.F. Vanderveen, F.J. Himpsel, D.E. Eastman, Phys. Rev., B 25 (1982) 7388.
[19] C.D. Wagner, A.V. Naumkin, A. Kraut-Vass, J.W. Allison, C.J. Powell, J.R. Rumble Jr., NIST Standard Reference Database 20, Version 3.4 (Web Version), National Institute of Standards and Technology, Gaithersburg, MD, 2000.
[20] B.V. Crist, Handbook of Monochromatic XPS Spectra Semiconductors, John Wiley and Sons, West Sussex, UK, 2000, p. 356.
[21] M. Zier, S. Oswald, R. Reiche, K. Wetzig, Anal. Bioanal. Chem. 375 (2003) 902.
[22] X. Zhao, N.P. Magtoto, M. Leavy, J.A. Kelber, Thin Solid Films 415 (2002) 308.
[23] B.R. Chakraborty, S. Hofmann, Thin Solid Films 204 (1991) 163.
[24] C.J. Powell, A. Jablonski, I.S. Tilinin, S. Tanuma, D.R. Penn, J. Electron. Spectrosc. 99 (1999) 1.
[25] J.F. Moulder, W.F. Stickle, P.E. Sobol, K.D. Bomben, W.F. Stickle, P.E. Sobol, K.D. Bomben, Handbook of X-ray Photoelectron Spectroscopy—A Reference Book of Standard Spectra for Identification and Interpretation of XPS Data, Physical Electronics, Eden Prairie, MN, 1995.
[26] C.J. Powell, A. Jablonski, NIST Electron Inelastic-Mean-Free-Path Database—Version 1.1, National Institute of Standards and Technology, Gaithesburg, MD, 2000.